

Are your **MRI contrast agents** cost-effective?

Learn more about generic **Gadolinium-Based Contrast Agents**.



**FRESENIUS  
KABI**

caring for life

**AJNR**

## **Advanced Fiber Tracking in Early Acquired Brain Injury Causing Cerebral Palsy**

F. Lennartsson, L. Holmström, A.-C. Eliasson, O. Flodmark, H. Forssberg, J.-D. Tournier and B. Vollmer

*AJNR Am J Neuroradiol* published online 28 August 2014  
<http://www.ajnr.org/content/early/2014/08/28/ajnr.A4072>

This information is current as of April 19, 2024.

# Advanced Fiber Tracking in Early Acquired Brain Injury Causing Cerebral Palsy

F. Lennartsson, L. Holmström, A.-C. Eliasson, O. Flodmark, H. Forssberg, J.-D. Tournier, and B. Vollmer



## ABSTRACT

**BACKGROUND AND PURPOSE:** Diffusion-weighted MR imaging and fiber tractography can be used to investigate alterations in white matter tracts in patients with early acquired brain lesions and cerebral palsy. Most existing studies have used diffusion tensor tractography, which is limited in areas of complex fiber structures or pathologic processes. We explored a combined normalization and probabilistic fiber-tracking method for more realistic fiber tractography in this patient group.

**MATERIALS AND METHODS:** This cross-sectional study included 17 children with unilateral cerebral palsy and 24 typically developing controls. DWI data were collected at 1.5T (45 directions,  $b=1000$  s/mm<sup>2</sup>). Regions of interest were defined on a study-specific fractional anisotropy template and mapped onto subjects for fiber tracking. Probabilistic fiber tracking of the corticospinal tract and thalamic projections to the somatosensory cortex was performed by using constrained spherical deconvolution. Tracts were qualitatively assessed, and DTI parameters were extracted close to and distant from lesions and compared between groups.

**RESULTS:** The corticospinal tract and thalamic projections to the somatosensory cortex were realistically reconstructed in both groups. Structural changes to tracts were seen in the cerebral palsy group and included splits, dislocations, compaction of the tracts, or failure to delineate the tract and were associated with underlying pathology seen on conventional MR imaging. Comparisons of DTI parameters indicated primary and secondary neurodegeneration along the corticospinal tract. Corticospinal tract and thalamic projections to the somatosensory cortex showed dissimilarities in both structural changes and DTI parameters.

**CONCLUSIONS:** Our proposed method offers a sensitive means to explore alterations in WM tracts to further understand pathophysiologic changes following early acquired brain injury.

**ABBREVIATIONS:** CerPed = cerebral peduncle; CP = cerebral palsy; CSD = constrained spherical deconvolution; CST = corticospinal tract; FA = fractional anisotropy; FTA = fiber-tract assessment; M1 = primary motor cortex; MD = mean diffusivity; PLIC = posterior limb of the internal capsule; TRS1 = thalamic projections to the somatosensory cortex

Cerebral palsy (CP) is a disorder of movement and posture caused by nonprogressive disturbances in the developing brain. Brain lesions that cause CP are commonly identified by visual inspection of conventional structural T1- and T2-weighted MR imaging. A range of macrostructural abnormalities has been

described.<sup>1</sup> However, subtle brain abnormalities may be missed on visual inspection.

Diffusion-weighted MR imaging can be used to infer the structural composition and integrity of neuronal tissue,<sup>2</sup> and white-matter fiber tractography can be used to trace fiber tracts noninvasively.<sup>3</sup> Diffusion tensor imaging describes a single diffusion process in a voxel. However, most voxels contain multiple, often crossing, fiber populations.<sup>4</sup> The use of probabilistic fiber tracking in diffusion models capable of resolving complex fiber struc-

Received February 26, 2014; accepted after revision July 5.

From the Department of Neuroradiology (F.L., O.F.), Karolinska University Hospital, Stockholm, Sweden; Departments of Clinical Neurosciences (F.L., O.F.) and Women's and Children's Health (L.H., A.-C.E., H.F., B.V.), Karolinska Institute, Stockholm, Sweden; The Florey Institute of Neuroscience and Mental Health (J.-D.T.), Melbourne, Victoria, Australia; Department of Medicine (J.-D.T.), University of Melbourne, Victoria, Australia; Centre for the Developing Brain (J.-D.T.) and Department of Biomedical Engineering (J.-D.T.), Division of Imaging Sciences and Biomedical Engineering, King's College London, London, United Kingdom; and Clinical Neurosciences, Clinical and Experimental Sciences (B.V.), Faculty of Medicine, University of Southampton, Southampton, United Kingdom.

This work was supported in part by grants from the Stockholm County Council (ALF project), the Swedish Medical Research Council, the Australian National Health and Medical Research Council, the Australian Research Council, and by a Marie Curie Fellowship for Experienced Researchers, FP6 Framework.

Please address correspondence to Finn Lennartsson, MD, Department of Neuroradiology, Karolinska University Hospital, SE-171 76 Stockholm, Sweden; e-mail: finn.lennartsson@karolinska.se

Indicates open access to non-subscribers at www.ajnr.org

Indicates article with supplemental on-line table.

Indicates article with supplemental on-line figure.

Evidence-Based Medicine Level 2.

<http://dx.doi.org/10.3174/ajnr.A4072>

tures is likely to be beneficial when studying white matter tracts and could provide additional information about the pathophysiology of altered fiber pathways. Findings in recent studies in CP support this assumption.<sup>5-7</sup>

In CP, studies have shown alterations in major fiber tracts, including the corticospinal tract (CST), the corticobulbar tract, superior and posterior thalamic radiations, the superior longitudinal fasciculus, and transcallosal fibers (for a review, see Scheck et al<sup>8</sup>). Parametric changes include decreased fractional anisotropy (FA) and increased mean diffusivity (MD), indicating altered tract microstructure. Decreased tract volumes and fiber counts, which may be indicative of perturbations during tract development, have been described.<sup>8</sup> Studies also have shown parametric changes that suggest secondary (Wallerian) neurodegeneration distant from the primary lesion site, with decreased FA and axial diffusivity (the largest tensor eigenvalue), increases in radial diffusivity (the mean of the 2 smaller tensor eigenvalues), but no changes or only slight increase in MD.<sup>5,9</sup> Moreover, the overall severity of CP, measured by, for example, the Gross Motor Function Classification System,<sup>10</sup> appears to correlate with diffusion parameters in motor<sup>9,11-13</sup> and/or sensory pathways.<sup>14-16</sup> In addition, correlations have been shown between diffusion measures in motor and sensory tracts and specific measures of sensory and/or motor functions.<sup>5-7,17-20</sup> Some studies suggest that sensory and motor functions correlate more strongly with changes in the sensory pathways (superior and posterior thalamic radiation) than changes in the motor pathways (CST).<sup>6,19</sup> These findings indicate that preservation of sensory pathways is important for motor function. However, most tractography studies in CP have used deterministic diffusion tensor tractography, which is a limitation because the algorithm cannot progress in areas where the tensor model shows a high uncertainty in the estimated fiber directions due to complex fiber architecture or pathologic changes.

In this study, we aimed to improve fiber tractography and characterization of motor and sensory fiber tracts in children with early acquired brain lesions by using a combined normalization and probabilistic fiber-tracking method. In addition, we aimed to use this method to characterize changes in gross morphology and in diffusion parameters close to and distant from the primary lesion.

## **MATERIALS AND METHODS**

### **Participants**

We examined a convenience sample of 17 children with unilateral spastic CP at the Gross Motor Function Classification System level I and the Manual Ability Classification System<sup>21</sup> levels I-II. After we excluded poor-quality imaging data, 15 children (6 boys, 9 girls; median age, 12.4 years; range, 7.2-17 years) remained in the sample (On-line Table). Twenty-four typically developing children served as controls (9 boys, 15 girls; median age, 12.7 years; range, 8.8-17.3 years; 23 right-handed). The lesion side is referred to as the hemisphere where structural abnormalities are detected on visual inspection of conventional structural MR imaging (On-line Table). In cases of bilateral lesions, the lesion side is defined as the most affected side as assessed by visual inspection. Measures from the lesion side in the subjects with CP are com-

pared with measures in the hemisphere ipsilateral to the dominant hand in the controls.

### **Neuroimaging**

MR imaging was performed on a 1.5T MR imaging system (Signa Excite Twinspeed; GE Healthcare, Milwaukee, Wisconsin). Conventional structural MR imaging included T1-, T2-weighted, and FLAIR images. DWI (TR/TE = 10,000/76 ms, voxel size = 2.3 mm<sup>3</sup> reconstructed to 1.72 mm<sup>2</sup> in-plane) included 6  $b = 0$  images followed by 45 gradient directions with  $b = 1000$  s/mm<sup>2</sup>. Conventional structural MRIs were visually assessed for lesion type, location, and extent. All controls had normal findings on MRI, and in the group with unilateral CP, a representative spectrum of lesions was seen (On-line Table).

### **Preprocessing of DWI**

Tools in the FSL package (Version 4.0; <http://www.fmrib.ox.ac.uk/fsl>)<sup>22</sup> were used for distortion and motion correction and to realign the gradient directions.<sup>23</sup> MRtrix (<http://neuro.debian.net/pkgs/mrtrix.html>)<sup>24</sup> was used for estimation of diffusion tensors and fiber orientation distributions with constrained spherical deconvolution (CSD) to assess multiple fiber populations in every voxel. From the diffusion tensors parametric maps of MD, FA, axial diffusivity, and radial diffusivity were computed.

All sections in all diffusion volumes and FA maps were visually inspected for artifacts. In addition, for each section, the mean signal was plotted over all diffusion volumes to detect large signal changes indicating gross imaging artifacts. Two of the original 17 subjects (1 child with a cortical malformation and 1 with white matter damage of immaturity) were excluded due to artifacts.

### **Spatial Normalization of DWI**

A study-specific FA template was created by using symmetric normalization.<sup>25</sup> A subset of 6 controls and 7 subjects (randomly selected after excluding subjects with a severe extent of WM damage and the patient with schizencephaly; On-line Table) were chosen for constructing the template. A  $b=0$  template and a color-coded FA template were constructed as the average of the corresponding images mapped into template space. All control and subject FA maps were then registered to this FA template. To check the consistency of the spatial registration, we mapped the FA template onto each subject's FA map by using the inverse transform. The results showed satisfactory agreement in the central and peripheral WM.

### **ROI Definition in Template Space**

Regions of interest in the cerebral peduncles (CerPeds), the posterior limb of the internal capsule (PLIC), the thalami, and the primary motor (M1) and somatosensory cortex were manually defined on the study template (On-line Fig).

### **ROI Mapping and Refinement**

All ROIs in template space were mapped onto each subject's native space. Transforming a binary region-of-interest image by using a continuous deformation field generates a nonbinary image in native space; therefore, the mapped region of interest had to be thresholded. Having explored several lower thresholds (0.1-0.5),

we chose a threshold of  $\geq 0.2$  to ensure anatomically adequate mapping of the template ROIs. Mapped ROIs were visually inspected and manually edited when required to ensure accurate anatomic placement. In addition, to prevent tracts from entering spaces with CSF, we multiplied the fiber-orientation distribution field by a subject-specific mask of the WM. The WM mask effectively confined the tracking to WM-dominated voxels but did not exclude any voxels in the thalami, for example.

### **Fiber Tracking of the Cortical Spinal Tract and the Thalamic Projections to the Somatosensory Cortex**

Probabilistic fiber tracking was performed on the CSD-estimated fiber orientation distribution fields with the mapped ROIs as input by using default tracking parameters. The CSTs were tracked by seeding in M1 and by using the PLIC and the cerebral peduncles on the same side as Waypoint masks. The thalamic projections to the somatosensory cortex (TRS1s) were tracked by seeding in the thalamus and by using the somatosensory cortex as a Waypoint mask. The fiber-tracking algorithm was run until  $10^4$  streamlines had been produced. Tracts that did not reach this number within  $10^8$  trials were considered to have an unrealistically low probability of connectivity and were excluded from further analysis.

Fiber tracts were converted to probability maps with voxel values equal to the fraction of the number of passing and generated streamlines. These were thresholded at 0.01 (1% of the total number of streamlines) and were considered to be the core of the fiber tracts. The ROIs for the PLIC and the cerebral peduncle were used to separate the CST probability maps into different parts: between M1 and the cerebral peduncle (CST-M1 to CerPed), between the PLIC and the cerebral peduncle (CST-PLIC to CerPed), and between M1 and the PLIC (CST-M1 to PLIC, not including PLIC-level voxels). The thalamic ROIs were used to remove thalamic voxels from the TRS1 probability maps. The complete processing from region-of-interest definition in the template space to the thresholded probability maps was performed twice in all participants by the primary study rater (F.L.) and, in a randomly selected subset of 7 subjects and 7 controls, by rater B.V., to evaluate the intra- and interrater reproducibility. To rule out partial volume effects as a confounder, we generated histograms of the MD voxel values in all probability maps; outliers were observed in only a very small proportion of voxels.

To assess diffusion parameters along CST and TRS1, we extracted the median voxel value (to minimize the influence of outliers) for FA and MD within the thresholded probability maps. In the CST-PLIC to CerPed, where the descending motor fibers are the dominating fiber population, the axial diffusivity and radial diffusivity were also extracted. For statistical comparisons, the mean of the median values for the trials of rater F.L. was used.

### **Qualitative Fiber-Tract Assessment**

From visual inspection of the fiber tracts, 4 distinct, spatial characteristics deviating from what is normally expected were identified in lesion-affected areas: dislocation of the major branch of the tract; local, continuous splitting of the tract into 2 separate

branches; compaction of a nonsplit tract; or failure to delineate the fiber tract (as described above). A fiber tract was found to have an atypical fiber-tract assessment (FTA) if  $\geq 1$  of these scenarios was observed along the tract and was confirmed on the thresholded probability map (Fig 1).

### **Statistics**

Statistical analyses were performed by using the Statistics Toolbox in Matlab (MathWorks, Natick, Massachusetts). To assess intra- and interrater reproducibility of fiber tracts, we performed pairwise comparisons of the spatial matching between the thresholded probability maps by calculating the Cohen  $\kappa$  coefficient.<sup>26</sup> Comparison of DTI parameters between subjects and controls was done by using the nonparametric Mann-Whitney  $U$  test (2-tailed, with  $P < .05$  as the significance threshold).

### **Ethics**

The study was granted ethics approval by the Regional Ethics Committee Stockholm North. All children and parents gave informed written consent.

## **RESULTS**

### **Reproducibility of Generated Fiber Tracts**

The normalization and fiber-tracking method showed high intra- and interrater reproducibility for all fiber tracts. Cohen  $\kappa$  values for the intrarater reproducibility were in the range of 0.88–0.98 for the controls and 0.81–0.94 for the subjects. For the interrater reproducibility, Cohen  $\kappa$  values were in the range of 0.84–0.91 for the controls and 0.87–0.92 for the subjects.

### **Applicability of the Fiber-Tracking Method in Typically Developing Controls**

Both the CST and the TRS1 were successfully reconstructed in agreement with expected neuroanatomy (column 1, Fig 1). In 3 controls the CST and in another 3 controls the TRS1 had atypical FTA with minor splits. None of the splits could be explained by any abnormalities on conventional structural MR imaging.

### **Applicability of the Fiber-Tracking Method in Subjects with Unilateral CP**

Both the CST and TRS1 were successfully reconstructed in most subjects with CP (On-line Table). On the nonlesion side, FTA for the TRS1 was typical for all subjects, whereas FTA for the CST was atypical in 1 subject having a minor split but without obvious underlying pathology (subject 5, On-line Table). In contrast, on the lesion side, the TRS1 and the CST showed atypical FTA in 7/15 and 10/15 subjects, respectively, and underlying pathologic changes were present in all these subjects (On-line Table). While atypical FTA was more frequently observed in the CST than in TRS1, in most cases, both tracts were affected simultaneously, though rarely in the same way.

### **DTI Parameters in Fiber Tracts**

Diffusion parameters (FA, MD, axial diffusivity, and radial diffusivity) for the CST and TRS1 were compared between the subjects with CP and the controls (Fig 2).

On the nonlesion side, both the CST-M1 to CerPed and its subsample CST-M1 to PLIC showed significant increases in MD

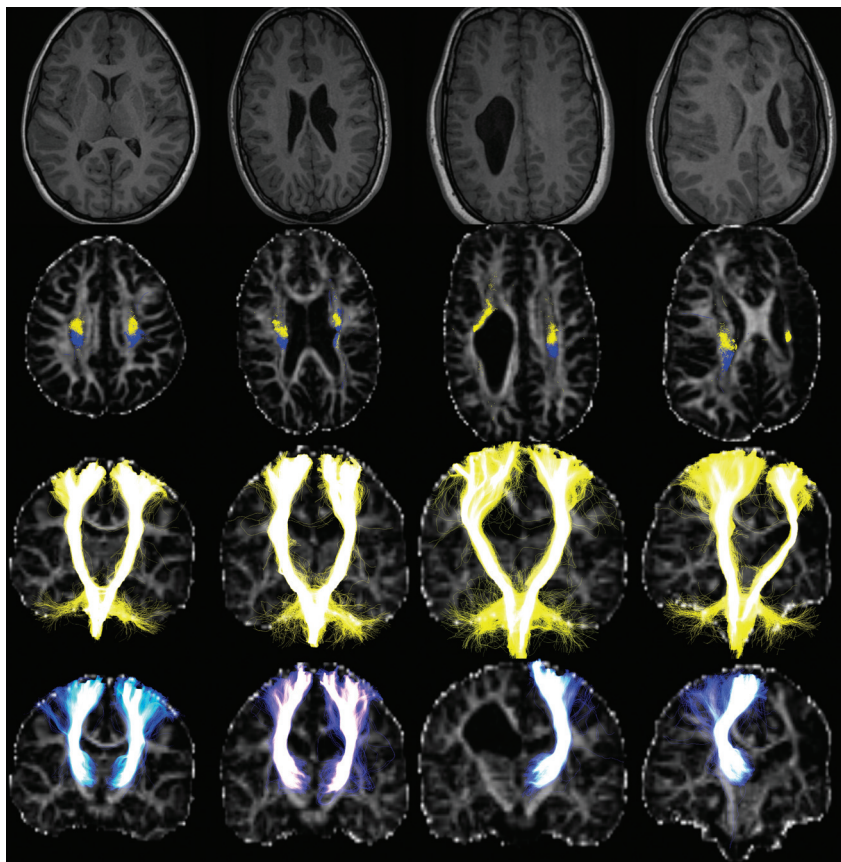


**FIG 1.** Tracking results of the CSTs (yellow) and the TRSIs (blue) in a healthy control (column 1) and 3 subjects with unilateral CP (columns 2–4, On-line Table). Images, shown in radiologic orientation, include T1-weighted images (row 1) and tracts superimposed on FA maps in the axial section at the level of the upper corona radiata (row 2) and entire coronal projections (rows 3–4). In the control (column 1), the CSTs are initiated from the entire M1 ROIs and follow consistent, expected paths down to the brain stem. The TRSIs are primarily initiated in the ventroposterior parts of the thalami, then travel posterior to the CSTs in the corona radiata, and spread over a large part of the somatosensory cortex ROIs. Subject 9 (column 2) has a periventricular pseudocyst at the level of corona radiata, which causes local splits to the left TRS1 and left CST, which are seen to partly share locations, and dislocate the major branch of the left CST. Subject 12 (column 3) has a large right WM lesion obstructing the anticipated courses of the TRSIs and the CSTs, making tracking of the TRS1 impossible and dislocating the right CST. Subject 14 (column 4) had a left focal infarct with extensive damage to the entire left hemisphere and severe WM damage above the PLIC, which confined the left CST to a thin sliver of WM at the level of the corona radiata and made the left TRS1 nontrackable.

( $P < .05$  and  $P < .05$ ) in the CP group compared with controls, whereas no changes in diffusion parameters were found in the subpart CST-PLIC to CerPed compared with controls. The TRS1 showed significant increase in MD ( $P < .05$ ) in the CP group compared with controls.

On the lesion side in the CP group with successful tracking of the CST ( $n = 12$ ), both CST-M1 to CerPed and CST-M1 to PLIC showed a significant decrease in FA ( $P < .001$  and  $P < .001$ ) and an increase in MD ( $P < .001$  and  $P < .001$ ) compared with controls. The subpart CST-PLIC to CerPed showed a significant decrease in FA ( $P < .001$ ) and axial diffusivity ( $P < .05$ ) and an increase in radial diffusivity ( $P < .001$ ) compared with controls. The TRS1 ( $n = 11$ ) showed a significant increase in MD ( $P < .01$ ) compared with controls.

## DISCUSSION

The CST and the TRS1 could be reconstructed according to expected neuroanatomy. We saw that DTI parameters varied along the CST in primary and secondary affected areas with traits consistent with primary and secondary (Wallerian) neurodegeneration. Both CST and TRS1 were affected on the lesion side; how-

ever, they showed different patterns on FTA assessment and in DTI parameters, which suggest that alterations were more pronounced in the CST than in the TRS1.

### Fiber-Tracking Method

Manually drawn ROIs have been used in most existing studies in CP, either for comparing diffusion parameters or as input for fiber tractography.<sup>8</sup> Often inter- and intrarater reproducibility statistics are reported, but ROIs may still not have been defined in comparable locations among subjects due to differences in section orientation. Defining ROIs on a normalized template could improve this deficiency. However, normalization of brains with lesions is difficult and has been used in few previous studies in CP.<sup>16,27,28</sup> In our study, the symmetric normalization algorithm<sup>25</sup> allowed accurate registration of central GM and WM, even in subjects with large brain lesions. The cortical GM and subcortical WM were less accurately registered, most likely due to intersubject variability in cortical sulcation patterns. Thus, the native-space ROIs of M1 and the somatosensory cortex had to be edited slightly in some individuals to ensure anatomically correct placement. Our sug-

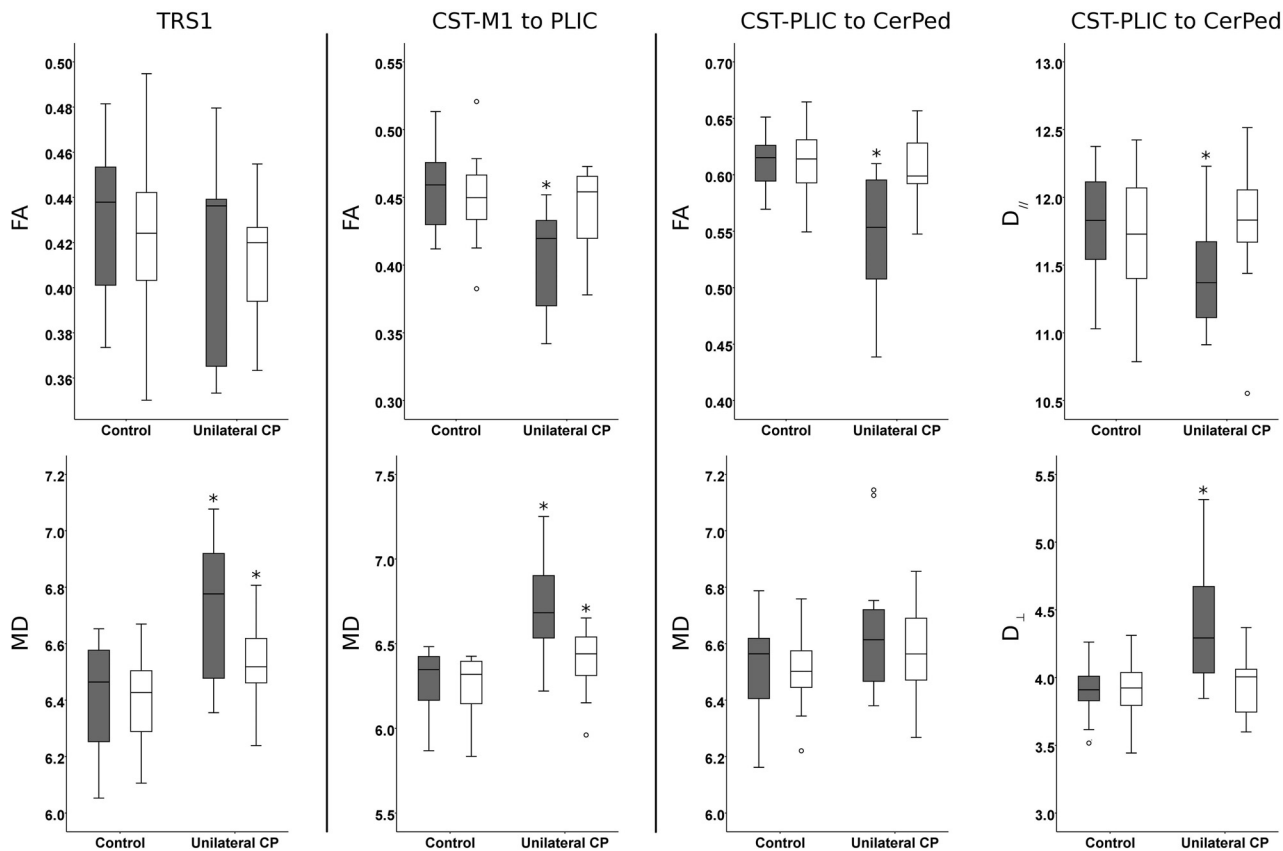


**FIG 2.** Boxplots of diffusion parameters in the TRS1, CST-M1 to PLIC, and CST-PLIC to CerPed in the group with unilateral CP and controls on the lesion (gray) and nonlesion (white) sides. Diffusivity is expressed as  $10^{-4}$   $\text{mm}^2/\text{s}$ . The asterisk indicates a significant difference between the group with unilateral CP and controls by statistical comparisons using the Mann-Whitney  $U$  test (2-tailed; significance level, .05).

gested method showed high intra- and interrater reproducibility, indicating that the method is robust.

Probabilistic fiber tracking with CSD of the CST and the TRS1 from their assumed starting points and including distant Waypoints appears to provide reliable and anatomically accurate tracking results. This finding is supported by Rose et al<sup>6</sup> and Tsao et al,<sup>7</sup> who also used probabilistic CSD fiber tractography to successfully track motor and sensory pathways. An alternative could have been to define the cortical ROIs from functional data such as fMRI. Thus, parts of the motor and somatosensory strips, such as the hand areas, could be targeted separately. However, the fMRI localization of functional areas is not perfect, the resolution is relatively poor, and it is not certain that fMRI would elicit a functional response in the CP group. Moreover, in early brain lesions, there are indications of different reorganizational patterns in the motor and somatosensory systems in CP. It has been shown that somatosensory functions show mainly ipsilesional reorganization patterns, whereas the motor functions can show ipsilesional, contralateral, or mixed reorganization patterns.<sup>29</sup> Functional MR imaging activation sites may therefore not be relevant as cortical targets because we were interested in the structure of the ipsi- and contralesional CST and TRS1.

Some case reports show diffusion tensor tractograms of thalamocortical connections that are displaced by lesions but still reach cortical areas in individuals with early acquired brain lesions (eg, Staudt et al<sup>30</sup>; Guzzetta et al<sup>31</sup>). With our method, we

observed, in several cases and in all lesion types, that both the CST and TRS1 on the lesion side have altered paths when passing lesion-affected areas. These fiber tracts showed expected distributions in their end points and displayed plausible deviations from their expected route, and both the CST and the adjacent TRS1 showed very similar but not identical behavior on FTA. Likewise, when a tract could not be delineated, the reason was, in all cases, an interruption of the tract by the lesion. At the same time, tracts on the nonlesion side followed paths consistent with those observed in the controls, indicating that the tracking method is robust.

#### Qualitative Fiber-Tract Assessment

We saw atypical FTA in many cases for both the CST and the TRS1 on the lesion side. The tracts that were classified as nontractable, compacted, or dislocated all corresponded with macrostructural abnormalities, but the splits detected were both plausible splits caused by the lesion and smaller splits that had no macrostructural correlate on conventional structural MR imaging. The occurrence of small splits without any macrostructural correlate might be explained by the limited performance of CSD with the current imaging protocol. Sampling more directions and using a larger  $b$ -value of 2000–3000  $\text{s}/\text{mm}^2$  would improve the ability of CSD to resolve the fiber-orientation distributions in cases of multiple fiber populations<sup>24</sup> but would make motion and eddy-current correction harder.

### DTI Parameter Changes in CST and TRS1

On the nonlesion side, the CST-PLIC to CerPed did not show any changes in DTI parameters, whereas farther up, both CST-M1 to PLIC and TRS1 showed similar significant increases in MD only, which were much less pronounced than on the lesion side. DWI increases the sensitivity of detecting lesions that commonly display increased MD. Our findings are suggestive of additional subtle lesions that can be detected with analysis of DTI parameters in patients without overt bilateral lesions on visual inspection of conventional structural MR imaging. A more speculative explanation may be secondary (Wallerian) neurodegeneration in these areas of intersecting pathways,<sup>32</sup> with involvement of transcallosal connections from the lesion side, which has been shown to be affected in CP.<sup>20</sup> In the future, it may be possible to investigate changes in the individual fiber populations in these areas by using parameters derived from multifiber models (eg, Raffelt et al<sup>33</sup>; Dell'Acqua et al<sup>34</sup>).

On the lesion side, the CST distant from the primary lesion site (CST-PLIC to CerPed) showed a pattern of diffusion measures indicative of secondary (Wallerian) neurodegeneration, whereas closer to the lesion, the CST-M1 to PLIC showed a pattern compatible with the signs of primary neurodegeneration.<sup>32</sup> This finding is in line with the results of Thomas et al,<sup>35</sup> who showed similar changes close to and distant from the lesion, and with Glenn et al<sup>9</sup> in their study of the CST between the PLIC and the cerebral peduncle. The TRS1 showed a significant increase in MD but no changes in FA, which do not indicate any specific pathologic pattern. Although the interpretation above of DTI parameters is the current prevailing view, there are several factors, both on a microscopic cellular and macroscopic architectural level, that will influence them and it is difficult to infer which factors actually account for a change.<sup>36</sup> Also, even if certain DTI changes are identified in a disease model, the inverse may not always hold; moreover, generalization of DTI changes from one disease model may not be valid in other situations. This is a potential problem in early brain lesions because we see a large spectrum of both lesions and etiologies. In our opinion, this issue remains unresolved. Many studies contain heterogeneous CP groups and/or lesion types.<sup>8</sup> Nevertheless, we did show that different parts of the CST display distinct patterns in DTI parameters, and extracting parameters as averages over large parts of the tracts, as done in most studies, might be misleading. Furthermore, on the lesion side, the TRS1 and the CST-M1 to PLIC both showed similar, significant increases in MD, but only CST-M1 to PLIC showed significant change in FA. The only study to report DTI parameters in both CST and superior thalamocortical fibers in unilateral CP is Thomas et al,<sup>35</sup> who also saw this distinction between FA and MD. The CST and TRS1 are affected differently in our patient cohort, as indicated by the FTAs and DTI parameters. We cannot infer the underlying cause of this difference from the limited information provided by DTI parameters in areas with complex fiber architecture. One speculative explanation could be that we see reactive changes in the somatosensory projections, and indeed, it has been proposed that there is a greater capacity for ipsilesional reorganization in the somatosensory system than in the motor system.<sup>29</sup>

### Limitations

Our sample is representative regarding the spectrum of lesion types in unilateral CP; however, the lesion groups are not equally represented. The study is partly limited by the fact that on the lesion side, we could not track the CST in 3/15 and TRS1 in 4/15 subjects with CP. Hence, we could not evaluate any DTI parameters along those tracts. It may have been possible to delineate more of these tracts by using an improved DWI protocol by increasing the number of diffusion directions and the b-value.

### CONCLUSIONS

We have successfully used a normalization method for improved region-of-interest definition and probabilistic CSD fiber tracking in individuals with early brain lesions and unilateral CP. Our study demonstrated structural changes in the CST and the TRS1 on the lesion side, which could be linked to underlying pathologic changes as seen on conventional structural MR imaging. Analysis of DTI parameters along the CST showed traits of primary neurodegeneration in lesion areas and distant secondary (Wallerian) neurodegeneration, emphasizing the importance of analyzing different parts of a tract separately. There were dissimilarities in both structural changes and in DTI parameters between the CST and TRS1 on the lesion side indicating differences in how a tract is affected by the injury. By providing sensitive means to, first, normalize and define ROIs and, second, to explore WM tracts in areas with complex white matter architecture, our methods improve interpretation of diffusion measures in early acquired brain lesions and, by inference, of underlying pathophysiologic changes.

Disclosures: Finn Lennartsson—*RELATED: Grant:* supported by grants provided by the Stockholm County Council (ALF project). Linda Holmström—*RELATED:* financed by one of the postgraduate programs at Karolinska Institute.\* Ann-Christin Eliasson—*UNRELATED: Grants/Grants Pending:* Swedish Research Council, Karolinska Institute, *Comments:* general grants including this study; *Stock/Stock Options:* Handfast AB, *Comments:* small agency for education (does not give stock dividends). Hans Forsberg—*UNRELATED: Board Membership:* scientific foundations, *Comments:* Center for Molecular Medicine, Sunnedahls Handikappfond; *Grants/Grants Pending:* Swedish Medical Research Council,\* Foundation Olle Engkvist Byggmästare,\* Swedish Brain Foundation,\* Foundation Frimurarna Barnhuset,\* Swedish Research Council (5925),\* Swedish Foundation for Strategic Research,\* Berzelii Center Stockholm Brain Institute (Vinnova and Swedish Research Council),\* Strategic Neuroscience Program at Karolinska Institute,\* Knut and Alice Wallenberg Foundation,\* and a research application to Promobilia (1 MSEK) pending\*; *Royalties:* Royalties are paid to me from Mac Keith Press, London, and from Studentlitteratur, Lund, for chapters in textbooks.\* Jacques-Donald Tournier—*RELATED: Grant:* Australian National Health and Medical Research Council,\* Australian Research Council.\* Brigitte Vollmer—*RELATED: Grant:* Marie Curie Fellowship for Experienced Researchers, FP6 Framework. \*Money paid to the institution.

### REFERENCES

1. Bax M, Tydeman C, Flodmark O. **Clinical and MRI correlates of cerebral palsy.** *JAMA* 2006;296:1602–08
2. Beaulieu C. **The basis of anisotropic water diffusion in the nervous system: a technical review.** *NMR Biomed* 2002;15:435–55
3. Mori S, Crain BJ, Chacko VP, et al. **Three-dimensional tracking of axonal projections in the brain by magnetic resonance imaging.** *Ann Neurol* 1999;45:265–69
4. Jeurissen B, Leemans A, Tournier JD, et al. **Investigating the prevalence of complex fiber configurations in white matter tissue with diffusion magnetic resonance imaging: prevalence of multifiber voxels in WM.** *Hum Brain Mapp* 2013;34:2747–66
5. Holmström L, Lennartsson F, Eliasson AC, et al. **Diffusion MRI in**

- corticofugal fibers correlates with hand function in unilateral cerebral palsy.** *Neurology* 2011;77:775–83
6. Rose S, Guzzetta A, Pannek K, et al. **MRI structural connectivity, disruption of primary sensorimotor pathways, and hand function in cerebral palsy.** *Brain Connect* 2011;1:309–16
  7. Tsao H, Pannek K, Boyd RN, et al. **Changes in the integrity of thalamocortical connections are associated with sensorimotor deficits in children with congenital hemiplegia.** *Brain Struct Funct* 2013 Oct 22. [Epub ahead of print]
  8. Scheck SM, Boyd RN, Rose SE. **New insights into the pathology of white matter tracts in cerebral palsy from diffusion magnetic resonance imaging: a systematic review.** *Dev Med Child Neurol* 2012;54:684–96
  9. Glenn OA, Ludeman NA, Berman JJ, et al. **Diffusion tensor MR imaging tractography of the pyramidal tracts correlates with clinical motor function in children with congenital hemiparesis.** *AJNR Am J Neuroradiol* 2007;28:1796–802
  10. Palisano R, Rosenbaum P, Walter S, et al. **Development and reliability of a system to classify gross motor function in children with cerebral palsy.** *Dev Med Child Neurol* 1997;39:214–23
  11. Kidokoro H, Kubota T, Ohe H, et al. **Diffusion-weighted magnetic resonance imaging in infants with periventricular leukomalacia.** *Neuropediatrics* 2008;39:233–38
  12. Murakami A, Morimoto M, Yamada K, et al. **Fiber-tracking techniques can predict the degree of neurologic impairment for periventricular leukomalacia.** *Pediatrics* 2008;122:500–06
  13. Rha D, Chang WH, Kim J, et al. **Comparing quantitative tractography metrics of motor and sensory pathways in children with periventricular leukomalacia and different levels of gross motor function.** *Neuroradiology* 2012;54:615–21
  14. Trivedi R, Agarwal S, Shah V, et al. **Correlation of quantitative sensorimotor tractography with clinical grade of cerebral palsy.** *Neuroradiology* 2010;52:759–65
  15. Yoshida S, Hayakawa K, Yamamoto A, et al. **Quantitative diffusion tensor tractography of the motor and sensory tract in children with cerebral palsy.** *Dev Med Child Neurol* 2010;52:935–40
  16. Lee JD, Park HJ, Park ES, et al. **Motor pathway injury in patients with periventricular leukomalacia and spastic diplegia.** *Brain* 2011;134:1199–210
  17. Bleyenheuft Y, Grandin CB, Cosnard G, et al. **Corticospinal dysgenesis and upper-limb deficits in congenital hemiplegia: a diffusion tensor imaging study.** *Pediatrics* 2007;120:e1502–11
  18. Ludeman NA, Berman JJ, Wu YW, et al. **Diffusion tensor imaging of the pyramidal tracts in infants with motor dysfunction.** *Neurology* 2008;71:1676–82
  19. Hoon AH Jr, Stashinko EE, Nagae LM, et al. **Sensory and motor deficits in children with cerebral palsy born preterm correlate with diffusion tensor imaging abnormalities in thalamocortical pathways.** *Dev Med Child Neurol* 2009;51:697–704
  20. Weinstein M, Green D, Geva R, et al. **Interhemispheric and intra-hemispheric connectivity and manual skills in children with unilateral cerebral palsy.** *Brain Struct Funct* 2014;219:1025–40
  21. Eliasson AC, Krumlinde-Sundholm L, Rösblad B, et al. **The Manual Ability Classification System (MACS) for children with cerebral palsy: scale development and evidence of validity and reliability.** *Dev Med Child Neurol* 2006;48:549–54
  22. Behrens TE, Berg HJ, Jbabdi S, et al. **Probabilistic diffusion tractography with multiple fibre orientations: what can we gain?** *Neuroimage* 2007;34:144–55
  23. Leemans A, Jones DK. **The B-matrix must be rotated when correcting for subject motion in DTI data.** *Magn Reson Med* 2009;61:1336–49
  24. Tournier JD, Calamante F, Connelly A. **MRtrix: diffusion tractography in crossing fiber regions.** *Int J Imaging Syst Technol* 2012;22:53–66
  25. Avants BB, Epstein CL, Grossman M, et al. **Symmetric diffeomorphic image registration with cross-correlation: evaluating automated labeling of elderly and neurodegenerative brain.** *Med Image Anal* 2008;12:26–41
  26. Landis JR, Koch GG. **An application of hierarchical kappa-type statistics in the assessment of majority agreement among multiple observers.** *Biometrics* 1977;33:363–74
  27. Faria AV, Hoon A, Stashinko E, et al. **Quantitative analysis of brain pathology based on MRI and brain atlases: applications for cerebral palsy.** *Neuroimage* 2011;54:1854–61
  28. Yoshida S, Faria AV, Oishi K, et al. **Anatomical characterization of athetotic and spastic cerebral palsy using an atlas-based analysis: anatomical characterization of cerebral palsy.** *J Magn Reson Imaging* 2013;38:288–98
  29. Guzzetta A, Bonanni P, Biagi L, et al. **Reorganisation of the somatosensory system after early brain damage.** *Clin Neurophysiol* 2007;118:1110–21
  30. Staudt M, Braun C, Gerloff C, et al. **Developing somatosensory projections bypass periventricular brain lesions.** *Neurology* 2006;67:522–25
  31. Guzzetta A, D'Acunto G, Rose S, et al. **Plasticity of the visual system after early brain damage: review.** *Dev Med Child Neurol* 2010;52:891–900
  32. Pierpaoli C, Barnett A, Pajevic S, et al. **Water diffusion changes in Wallerian degeneration and their dependence on white matter architecture.** *Neuroimage* 2001;13:1174–85
  33. Raffelt D, Tournier JD, Rose S, et al. **Apparent fibre density: a novel measure for the analysis of diffusion-weighted magnetic resonance images.** *Neuroimage* 2012;59:3976–94
  34. Dell'Acqua F, Simmons A, Williams SC, et al. **Can spherical deconvolution provide more information than fiber orientations? Hindrance modulated orientational anisotropy, a true-tract specific index to characterize white matter diffusion.** *Hum Brain Mapp* 2013;34:2464–83
  35. Thomas B, Eyssen M, Peeters R, et al. **Quantitative diffusion tensor imaging in cerebral palsy due to periventricular white matter injury.** *Brain* 2005;128(pt 11):2562–77
  36. Wheeler-Kingshott CA, Cercignani M. **About “axial” and “radial” diffusivities.** *Magn Reson Med* 2009;61:1255–60